Metathesis Activity and Properties of Mo−Alkylidene Sites Differently Located on Silica. A Density Functional Theory Study

Jarosław Handzlik*

Institute of Organic Chemistry and Technology, Cracow University of Technology, ul. Warszawska 24, PL 31-155 Kraków, Poland

Received: June 28, 2005; In Final Form: September 5, 2005

Ethene metathesis proceeding on Mo−methylidene centers on silica is investigated with density functional theory, applying the cluster approach. Three different locations of the active sites are considered, in which the Mo center replaces a pair of geminal silanols, two silanols from adjacent geminal pairs and two single silanols, respectively. It is shown that metathesis activity of the Mo−methylidene sites strongly depends on their location on silica. Different reactivity of the centers toward alkene is explained by differences in their geometrical and electronic structure parameters. The calculated C−H stretching vibrations of the proposed Mo−methylidene, Mo−ethylidene, and molybdacyclobutane surface complexes are well consistent with the reported IR spectra for the corresponding species generated on real molybdena−silica catalysts. On the basis of the obtained results it is proposed that among the studied cases, the Mo centers replacing two silanols from adjacent geminal pairs of silica surface are the most adequate models of the real active sites.

1. Introduction

Supported Mo systems are of importance in a variety of catalytic processes, which include olefin metathesis.[1,2] Among the heterogeneous molybdena catalysts, molybdena−silica systems can exhibit an excellent metathesis activity if a suitable preparation and activation procedure is applied.[1,3−13] The photoreduced molybdena−silica systems were comprehensively investigated in olefin metathesis.[4−11] Unlike most of the heterogeneous metathesis catalysts, the concentration of the active sites in the photoreduced systems treated with cycloalkane is high. This enabled spectroscopic studies that confirmed the presence of Mo−alkylidene and molybdacyclobutane species on the catalyst surface.[5−7,10] Such structures are postulated within the commonly accepted carbene mechanism of olefin metathesis, first proposed for the homogeneous catalysts.[14,15] According to this mechanism, the metal−alkylidene complex reacts with an olefin molecule giving a metallacyclobutane intermediate that decomposes to a new metal−alkylidene structure and another olefin molecule.

It was experimentally shown for the alkylidene Schrock catalysts, Mo(NAr)(CHR)(OR′)$_2$ and W(NAr)(CHR)(OR′)$_2$, that the metallacyclobutane complexes, formed during olefin metathesis process, possess either trigonal bipyramidal (TBP) or square pyramidal (SP) geometry. Both the stability of the given metallacyclobutane type and the activity of the catalyst are governed, among other factors, by electronic properties of the alkoxide ligands.[16−22] Theoretical studies of the corresponding Mo model systems[23−25] confirmed that the relative electron-withdrawing OR′ groups lower the activation barrier of alkene addition to the Mo−alkylidene complex and stabilize the TBP molybdacyclobutane.

In the case of the supported catalysts, the carrier can be considered as a ligand of the metal center.[26,27] Therefore, analogously to the homogeneous metathesis catalysts, the local properties of the support should influence the reactivity of the active sites. Indeed, our previous theoretical work concerning heterogeneous molybdena−alumina systems[28,29] proved that location of the monomeric Mo−alkylidene center on γ-alumina affects its reactivity toward alkene. Both local electronic properties of the carrier and geometry of the active site, the factors depending on the Mo center location, influence the activation barriers, as well as the stabilities of the molybdacyclobutane intermediates.

A crucial problem involved in theoretical investigations of heterogeneous catalytic processes is modeling of the geometry of the surface active sites. Most of the spectroscopic data show that monomeric oxide Mo^{VI} sites on MoO_3/SiO_2 catalyst have tetrahedral geometry.[30−42] Many authors proposed that these centers are dioxo ones.[3,4,6,10,30−32,35−42] Other results indicate the presence of monooxo, not dioxo, surface monomeric Mo^{VI} species on silica, under dehydrated conditions.[43−46] Although Mo^{V} sites with distorted square pyramidal configuration were postulated to be responsible for metathesis activity,[1,47,48] there is strong experimental evidence that reduced Mo^{IV} forms are the precursors of the active metathesis sites on silica.[1,3−10,35,49] In the latter case, monooxo Mo^{IV} species replacing two silanol groups are proposed as the precursors. As concerns monomeric Mo−alkylidene sites on silica, distorted tetrahedral centers replacing two silanols and having the oxo ligand and the alkylidene ligand (Figure 1) are generally suggested.[1,3,6−10,36] Such structures are analogous to the above-mentioned, very efficient pseudotetrahedral Schrock catalysts.[16−22] On the other hand, to the best of my knowledge, any theoretical studies of Mo−alkylidene sites on silica have not been reported, so far.

The purpose of the present work is a theoretical investigation of ethene metathesis activity of Mo−methylidene centers on silica. Advanced cluster models are applied to model the silica surface. Three different locations of the active sites are considered and the influence of the Mo−methylidene center position on its activity is discussed, considering both electronic properties and geometrical parameters of the site. Additionally,

* Corresponding author: tel, +48-12-6282761; fax, +48-12-6282037; e-mail, jhandz@usk.pk.edu.pl.

10.1021/jp053517b CCC: $30.25
Published on Web 10/19/2005

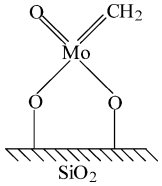

Figure 1. The proposed structure of the Mo−methylidene site on silica.[1,3,6−10,36]

the calculated vibrational frequencies of the considered Mo−methylidene, Mo−ethylidene, and molybdacyclobutane surface species are compared with the reported IR spectra for the real molybdena−silica metathesis catalysts.

2. Models of Silica Surface

The high surface area silica is an amorphous material, and modeling its surface is a difficult task. On the basis of ^{29}Si NMR, ^{1}H NMR, and IR results, both geminal and single as well as hydrogen-bonded and isolated silanols are distinguished on the silica surface.[50−58] It was reported that the structure of amorphous silica resembles that of β-cristobalite, and the kinds and concentration of the surface hydroxyl groups on silica and on β-cristobalite are also similar.[50,51,54,55] Therefore, many theoretical simulations of amorphous silica are based on the β-cristobalite structure.[59−71] On the fully hydroxylated (100) plane of β-cristobalite, all the silanols are of geminal type. Hydroxyl groups of adjacent geminal pairs can form hydrogen bonds, which facilitate partial dehydroxylation at elevated temperatures, leading to siloxane linkages and isolated hydroxyls, so-called vicinal
silanols.[50,51,54,55,60−62,66] On the other hand, only isolated single hydroxyl groups can be present on the (111) surface of β-cristobalite.[50,51,54,55,61,66] It is proposed that real silica surface contains segments resembling both (100) and (111) faces of β-cristobalite.[50,54,55]

Although the structure of β-cristobalite is commonly analyzed in the cubic *Fd*3*m* space group,[72−76] it can be interpreted as corresponding to the average structure of domains of lower symmetry, described by the tetragonal $I\bar{4}2d$ space group.[62,75,76] In the present work, the $I\bar{4}2d$ structure of β-cristobalite[75] with Si in 4(a) and O in 8(d) crystallographic positions was used to model silica. Three cluster models of silica surface, denoted as **a**, **b**, and **c** (Figure 2) are cut out from the crystal structure. The dangling bonds of the silica clusters have been saturated with hydrogens, placed 0.97 Å from oxygen atoms along the O−Si bond direction of the perfect crystal. This technique is commonly adopted, specially for clusters of covalent materials. The upper parts of the cluster models, including five, six, and eight Si atoms for **a**, **b**, and **c**, respectively, were relaxed.

Both **a** and **b** silica clusters model the (100) face of β-cristobalite, while the **c** cluster represents the (111) surface. For better clarity, the notation of the crystallographic planes is referred to the *Fd*3*m* space group. In cluster **a**, geminal silanol pairs are exposed (Figure 2). Cluster **b** models two surface silanols, coming from adjacent geminal pairs. After relaxation of the surface, a hydrogen bond is formed between these hydroxyl groups, what is indicated by the O···H distance of 1.835 Å. This is in accordance with both experimental[54,55] and theoretical[62,66] results that confirmed formation of hydrogen bonds between adjacent geminal silanols. Finally, a silica surface with single, isolated hydroxyls is modeled using structure c (Figure 2). Previously,[29] it was shown that a cluster containing eight Al atoms is an adequate model to represent the surface of

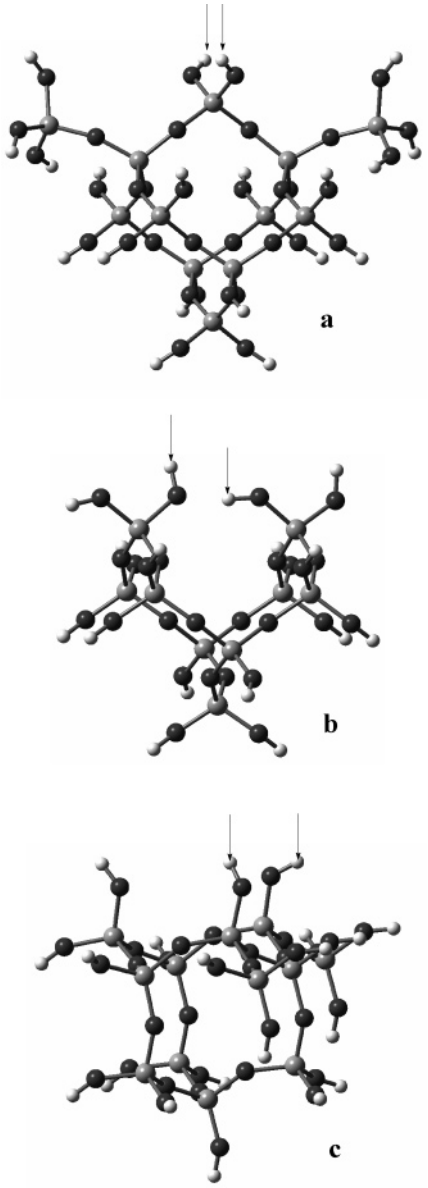

Figure 2. Cluster models of SiO_2 after relaxation of the surface part.

γ-Al_2O_3, which is a more ionic material than silica. Taking into account the size of the presently proposed clusters (9 or 12 Si atoms), it seems that they are large enough for realistic modeling of SiO_2, assuming β-cristobalite as a suitable model of the silica surface.

Proposed models of Mo−methylidene and Mo−ethylidene centers have been attached to the clusters **a**−**c**, by replacing the respective pairs of silanols (indicated by the arrows in Figure 2). The geometries of the active sites have been optimized together with the defined above surface parts of the silica clusters. The positions of other atoms and the terminating hydrogens were frozen.

3. Computational Details

DFT calculations were done with using the hybrid B3LYP functional[77,78] and the GAUSSIAN 03[79] set of programs. The LANL2DZ basis set including the Hay−Wadt effective core potential[80] plus double-ζ basis was used to describe molybdenum. For C, H, O, and Si the Dunning−Huzinaga full double-ζ basis set (D95)[81] was applied. This basis combination, denoted here as A, was applied for geometry optimization, carried out

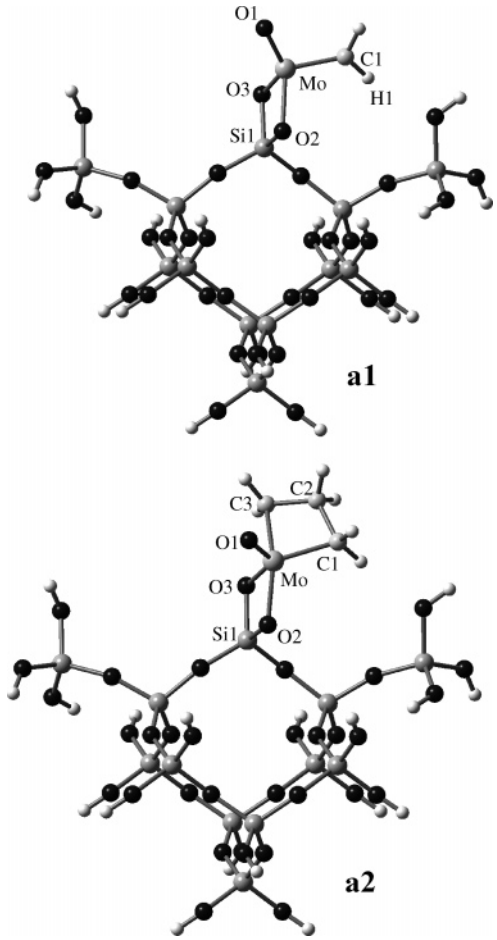

Figure 3. Optimized structure of the Mo−methylidene site replacing the geminal silanols on the silica surface (**a1**) and the corresponding molybdacyclobutane intermediate (**a2**).

by employing the Berny algorithm and redundant internal coordinates.[82] The potential energy minima and the localized transition states were confirmed by analysis of harmonic vibrational frequencies. The zero-point energy (ZPE) corrections were calculated for each structure. The Gibbs free energies of reactions at 298.15 K and 1 atm were estimated by treating the whole models as ideal gas molecules.

Single point energy calculations for the optimized structures were performed using the D95(d,p) basis for C, O, Al, and H, combined with the LANL2DZ basis for Mo (the basis combination denoted as B). The presented relative energies were calculated according to the B3LYP/B//B3LYP/A scheme. All the energy values are ZPE corrected.

To analyze the O−H stretching vibrations, the geometries of the silica cluster models were optimized at the B3LYP/6−31g-(d) level and then the harmonic vibrational frequency calculations were done.

Electronic properties of the active centers are discussed on the basis of the B3LYP/B//B3LYP/A calculations using the Mulliken population analysis (MPA),[83] the natural population analysis (NPA) together with the natural bond orbital analysis (NBO),[84,85] and the Mayer bond-order indices.[86]

4. Ethene Metathesis on Mo−Methylidene Centers on Silica

4.1. Mo−Methylidene Site Replacing the Pair of Geminal Silanols. In Figure 3, the structure of the Mo−methylidene center **a1**, obtained after the geometry optimization, is presented.

TABLE 1: Selected Bond Lengths (Å) for the Mo−Methylidene Center a1 and the Molybdacyclobutane Intermediate a2[a]

	a1		
		P	a2
Mo−C1	1.892	1.65	2.036
Mo−C3			2.108
Mo−O1	1.719	1.99	1.722
Mo−O2	1.993	0.85	1.947
Mo−O3	1.970	0.87	2.103
C1−C2			1.638
C2−C3			1.578
O2−Si1	1.741	0.88	1.749
O3−Si1	1.742	0.88	1.701

[a] For the former structure, the bond-order indices (*P*) are also listed.

TABLE 2: Selected Bond Lengths (Å) for the Mo−Methylidene Center b1 and the Respective Intermediates and Transition States Involved in Ethene Metathesis[a]

	b1					
		P[a]	b2	b3	b4	b5
Mo−C1	1.894	1.69	1.944	2.082	2.059	2.199
Mo−C3			2.329	2.086	2.152	2.194
Mo−O1	1.716	2.01	1.738	1.745	1.722	1.717
Mo−O2	1.910	0.75	1.923	1.898	1.923	1.912
Mo−O3	1.892	0.70	1.967	1.974	1.965	1.896
C1−C2			2.258	1.616	1.603	1.536
C2−C3			1.426	1.611	1.577	1.535
O2−Si1	1.683	0.96	1.667	1.672	1.667	1.675
O3−Si2	1.663	0.99	1.656	1.655	1.664	1.661

[a] For the former structure, the bond-order indices (*P*) are also listed.

The Mo center has replaced the geminal silanols pair from the silica cluster model **a**; therefore the molybdenum is connected via two oxygen atoms with one silica atom. Addition of ethene molecule to center **a1** leads to formation of molibdacyclobutane intermediate **a2** (Figure 3). This is the only intermediate structure that has been localized on the potential energy surface (PES). Selected bond lengths and bond orders for the Mo−methylidene and molybdacyclobutane centers are listed in Table 1. The predicted Mo−C1 distance in **a1** is close to the carbene bond length of the four-coordinate Mo−alkylidene complex (1.880 Å),[17,19] as well as to the calculated Mo═C lengths for Mo−methylidene centers replacing bridge hydroxyl groups on alumina.[28,29] The Mo═C bond order for **a1** is also very similar to the previously calculated values for the Mo−methylidene sites on alumina.[28,29] The NBO analysis confirms that one σ and one π bond contribute to the overall Mo═C bond. In the σ-NBO, 37% of the charge is polarized toward the Mo, while in the π-NBO the electron density is almost equally distributed between both atoms (52% toward the Mo). This can be interpreted in the terms of predominantly dative carbon to molybdenum σ bond and covalent Mo−C π bond.[87]

The O−Si bond orders are higher than the indices obtained for the corresponding O−Al bonds on (100) γ-Al_2O_3 (0.78),[29] indicating, as one could expect, more covalent bonding in the first case (see also the corresponding values in Tables 2 and 3). The respective values from Table 1 are consistent with the formally double Mo−O1 bond and single both Mo−O2 and Mo−O3 ones. However, the NBO analysis gives in the first case one σ-NBO and two π-NBOs, indicating a pseudo triple Mo−O1 bond, since one of the oxygen electron pairs is donated to the metal center.[21,88] The results of the NBO analysis of other studied Mo−methylidene centers are analogous.

Formation of the molybdacyclobutane structure **a2** from the Mo−methylidene center **a1** and ethene is a clearly exothermic

TABLE 3: Selected Bond Lengths (Å) for the Mo−Methylidene Center c1 and the Respective Intermediates and Transition States Involved in Ethene Metathesis[a]

	c1					
		P	c2	c3	c4	c5
Mo−C1	1.888	1.70	1.938	2.090	2.057	2.197
Mo−C3			2.336	2.078	2.183	2.201
Mo−O1	1.707	2.05	1.730	1.735	1.732	1.720
Mo−O2	1.956	0.72	1.974	1.945	1.976	1.969
Mo−O3	1.947	0.68	2.037	2.042	1.963	1.940
C1−C2			2.342	1.612	1.601	1.531
C2−C3			1.418	1.618	1.564	1.531
O2−Si1	1.690	1.00	1.680	1.688	1.721	1.703
O3−Si2	1.690	1.00	1.687	1.686	1.712	1.710

[a] For the former structure, the bond-order indices (*P*) are also listed.

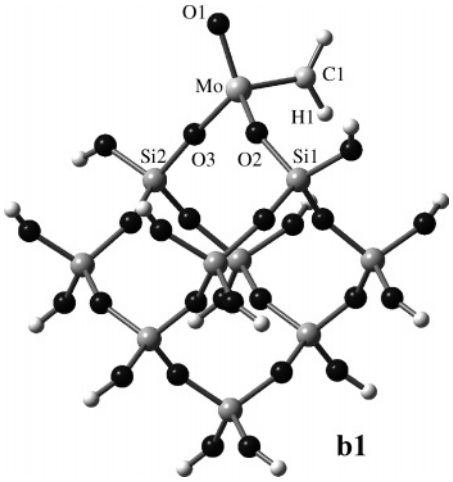

Figure 4. The optimized structure of the Mo−methylidene site replacing two silanols from the adjacent geminal pairs on the silica surface.

process with the predicted energy change of −84 kJ·mol^{-1}. Approximately the same energy barrier must be involved in decomposition of **a2** into a new Mo−methylidene complex and ethene molecule, which is necessary to continue the catalytic cycle of ethene metathesis. The estimated Gibbs free energy of reaction: **a1** + C_2H_4 → **a2** is −31 kJ·mol^{-1} (B3LYP/B//B3LYP/A). Therefore, the molybdacyclobutane site **a2** is a relatively stable species. Consequently, the Mo−methylidene center **a1**, although exhibiting high reactivity toward ethene, seems to have low activity in the overall metathesis process, at least at lower temperatures.

During ethene addition to the **a1** center a stable alkene complex is probably not formed or exists as a very shallow minimum on the PES—several attempts to optimize the geometry of such a structure have finished in obtaining the molybdacyclobutane **a2**. Also, many trials to localize the transition state on the PES have been unsuccessful. It seems that the molybdacyclobutane complex **a2** is formed practically without the energy barrier.

4.2. Mo−Methylidene Site Replacing Two Silanols from Adjacent Geminal Pairs. In Figure 4, the optimized structure of Mo−methylidene complex **b1**, in which the Mo center has replaced two hydroxyl groups from the adjacent geminal pairs, is shown. Selected bond lengths and bond orders for this structure are listed in Table 2. Among the studied Mo−methylidene centers, the Mo−O2 and Mo−O3 distances for **b1** are the closest to the experimentally determined single Mo−O bond length (1.87−1.88 Å) for the surface monomeric Mo^{VI} oxide species on silica.[41,42]

After addition of ethene to the Mo−methylidene center **b1**, the TBP molybdacyclobutane **b3** is formed, via the transition state **b2** (Figure 5). Previous calculations for the molybdena−alumina system[28,29,89−91] also showed that the TBP intermediate is a first product of alkene addition to Mo−alkylidene center, excluding an alkene−molybdenaalkylidene complex, which is formed, in some cases, at the early stage of the reaction.[28,29] In the next step of ethene metathesis, the TBP intermediate **b3** decomposes to a new [Mo]═$C3H_2$ surface complex and ethene molecule $C1H_2$═$C2H_2$. However, because of approximate symmetry of the molybdacyclobutane ring, this step is expected to be very similar to the reverse reaction: **b3** → **b1** + C_2H_4. Therefore, the additional calculations were not undertaken.

The TBP intermediate can also rearrange to the molybdacyclobutane **b5** (Figure 5). This transformation, involving the transition state **b4**, can be described as a pseudorotation of the molybdacyclobutane ring.[90] The **b5** structure has a little deformed SP geometry. The bond lengths of the ring in the considered transition state and the SP site (Table 2) are close to the corresponding values calculated for the analogous structures placed on alumina.[28,29,89−91] The Mo−C distances for **b5** are also similar to those experimentally obtained for the isolated SP molybdacyclobutane complex (2.211 and 2.227 Å).[18] Degradation of the SP molybdacyclobutane to the respective Mo−methylidene center and ethene proceeds via the TBP intermediate,[89−91] so the conversion of the TBP intermediate into the SP structure can be treated as a side step in the catalytic cycle.

According to the applied level of theory, the formation of the TBP molybdacyclobutane **b3** from the Mo−methylidene site **b1** and ethene is a slighty endothermic process (Figure 6) with high positive change of Gibbs free energy (58 kJ·mol^{-1}). The calculated activation energy is moderate (37 kJ·mol^{-1}) and the energy barrier of decomposition of the TBP intermediate to metathesis products is even lower (about 32 kJ·mol^{-1}). For the photoreduced molybdena−silica catalyst, which was highly active in propene metathesis at low temperatures, the apparent activation energy of 20 kJ·mol^{-1} was estimated from the kinetic data.[4] Even the lower values (5−11 kJ·mol^{-1}) were reported for catalysts prepared by fixation of Mo allyl complexes on SiO_2.[3] In the case of molybdena−alumina systems, the reported apparent activation energies of propene metathesis are in the wide range of 7−37 kJ·mol^{-1}. [3,92−95] However, only few data concerning the true activation energy are available. For propene metathesis on $MoO_3/CoO/Al_2O_3$ catalyst, the value of 34 kJ·mol^{-1} (the apparent activation energy of 23 kJ·mol^{-1}) was obtained, applying the Langmuir−Hinshelwood model.[96] A kinetic model of propene metathesis, derived from the carbene mechanism, was used in the case of a highly active at room temperature Re_2O_7/Al_2O_3 system, giving the true and apparent activation energy of 41 and 19 kJ·mol^{-1}, respectively.[97] Therefore, one can state that the present energy results are well consistent with the experimental data. This justifies the proposed Mo−methylidene center **b1** as an adequate model of the active metathesis site.

The rearrangement of the TBP molybdacyclobutane **b3** into the SP isomer **b5** is a clearly exothermic step (Figure 6) with the calculated value of $\Delta G = -60$ kJ·mol^{-1}. However, the predicted energy barrier of this transformation (44 kJ·mol^{-1}) is higher than the activation energy of the TBP intermediate decomposition to the metathesis products. Thus, ethene metathesis is kinetically favored over the conversion of the TBP intermediate to the SP structure. This is a significant difference,

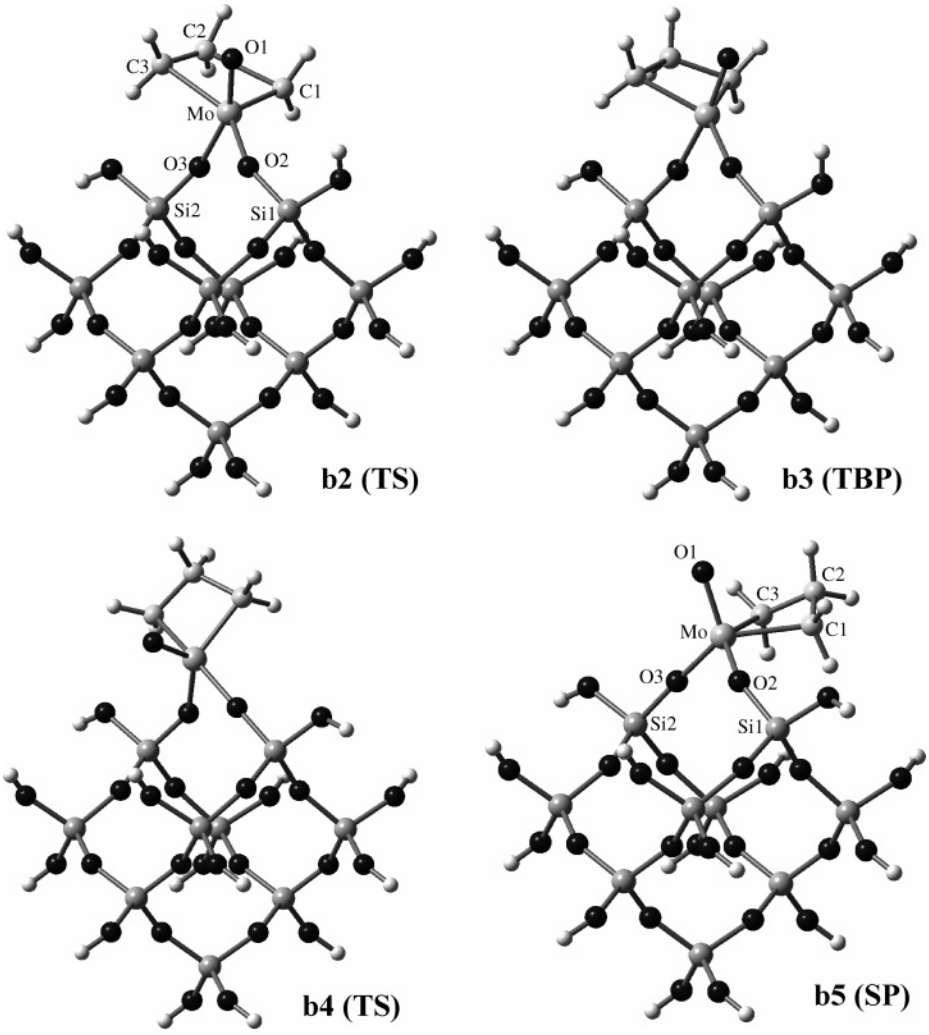

Figure 5. The minima (**b3**, **b5**) and the transition states (**b2**, **b4**) involved in the pathway of ethene metathesis on the Mo−methylidene center **b1**.

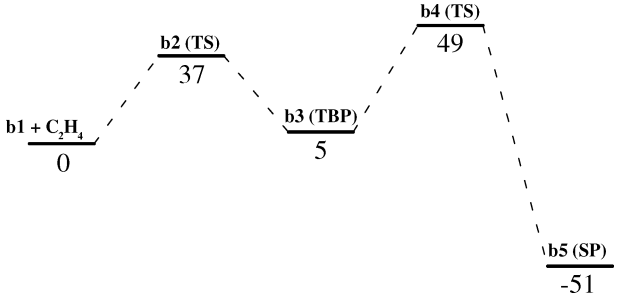

Figure 6. Energy diagram of ethene metathesis on the Mo−methylidene center **b1**. The relative energies (kJ·mol^{-1}) are obtained from the B3LYP/B//B3LYP/A calculations.

if compared to the theoretical results obtained earlier for the molybdena−alumina systems, where, in most cases, the formation of the stable SP molybdacyclobutane is kinetically preferred over the decomposition of the TBP intermediate to the metathesis products.[28,29,89−91] The back rearrangement of the SP molybdacyclobutane **b5** to the TBP one is connected with high energy barrier of 100 kJ·mol^{-1}. On the other hand, the estimated Gibbs free energy of the overall reaction: **b1** + C_2H_4 → **b5** is close to zero (−2 kJ·mol^{-1}), indicating possible thermodynamic equilibrium between the reactants and the SP intermediate. Ethene excess shifts this equilibrium toward the SP molybdacyclobutane. Therefore, the side reaction **b3** → **b5** can be considered as a reversible deactivation route, at least at lower temperatures of the process, when the reverse step is kinetically hindered. Among many possible reasons for experimentally observed intrinsic deactivation of the supported Mo catalysts of olefin metathesis, the most probable is reductive elimination of the molybdacyclobutane intermediate.[1,10] However, transformation of the very reactive TBP structure to the stable SP molybdacyclobutane complex can also, at least to some extent, explain decrease of the catalyst activity during the process.

4.3. Mo−Methylidene Site Replacing Two Single Silanols. The structure of the Mo−methylidene center **c1** that replaces two single silanols is shown in Figure 7. The optimized geometrical parameters and bond orders are given in Table 3.

The reaction path of ethene metathesis on the **c1** site is fully analogous to the pathway described for the **b1** center. In Figure 8, the TBP (**c3**) and SP (**c5**) molybdacyclobutane intermediates and the transition states involved (**c2** and **c4**, respectively) are presented. Comparing the geometries of the minima and transition states of both reaction paths (Tables 2 and 3), one can notice close analogy. The exceptions are the single Mo−O bonds, clearly longer in the **c** series compared to the **b** series. This is a consequence of a bigger distance between the silanol groups in the **c1** model of the SiO_2 surface. Another difference is a small interaction between the O1 atom and a hydrogen atom from the adjacent surface silanol, observed in the case of the **c4** and **c5** structures (Figure 8). The SP molybdacyclobutane, in which the OH group does not interact with the O1 atom, has been also localized. Its geometrical parameters are very close to those of **c5**.

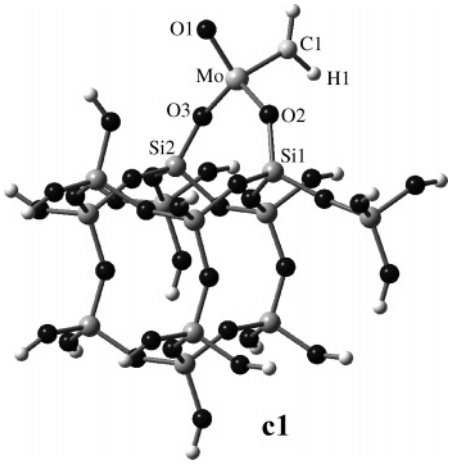

Figure 7. The optimized structure of the Mo−methylidene site replacing two single silanols.

The TBP molybdacyclobutane **c3** is formed in an endothermic step (Figure 9) and is even less stable, related to the reactants ($\Delta G = 73$ kJ·mol^{-1}), than the corresponding intermediate **b3**. The predicted activation energy of this step is higher, compared to the pathway involving the Mo−methylidene center **b1**. What is important, the calculated energy barrier of the rearrangement of the TBP intermediate **c3** to the SP molybdacyclobutane **c5** (61 kJ·mol^{-1}) is still higher than the activation energy of the degradation to the Mo−methylidene and ethene (37 kJ·mol^{-1}). Thus, the latter step is kinetically favored and the considered difference in the energy barrier of both competitive steps is even larger than that in the case of the **b3** intermediate. On the other hand, the SP molybdacyclobutane **c5** has still the lowest energy on the PES and its transformation to the TBP intermediate involves an activation barrier of 129 kJ·mol^{-1} (Figure 9). Similarly as in the case of the pathway starting from the **b1** center, the estimated value of ΔG for the reaction: **c1** + C_2H_4 → **c5** is close to zero (8 kJ·mol^{-1}).

In conclusion, the considered Mo−methylidene center **c1** is predicted to be less active in ethene metathesis, compared to the **b1** structure; however, it is still a reasonable candidate for the metathesis active site, especially at higher temperatures.

5. Factors Determining the Reactivity of the Mo−Methylidene Centers

In Table 4, both electronic and selected geometrical parameters of the Mo−methylidene sites are compared. In the last two rows of the table, the energies and activation energies of the formation of the first molybdacyclobutane intermediate are shown. Both quantities closely relate to reactivity of the considered centers toward ethene. On the basis of the obtained results, the reactivity order of the studied Mo−methylidene centers is as follows:

$$\mathbf{a1} \gg \mathbf{b1} > \mathbf{c1}$$

Reduced electron density on the active site should facilitate nucleophilic attack of ethene. Thus, one could expect higher

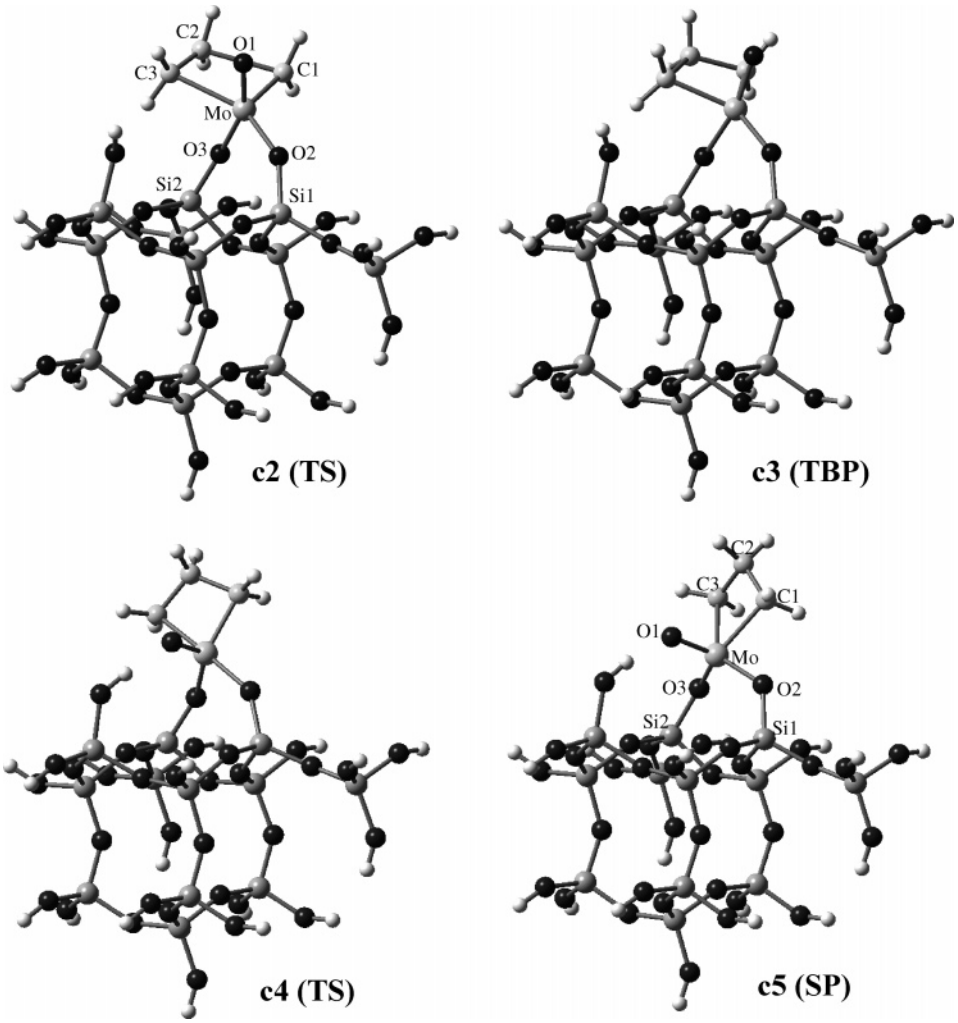

Figure 8. The minima (**c3**, **c5**) and the transition states (**c2**, **c4**) involved in the pathway of ethene metathesis on the Mo−methylidene center **c1**.

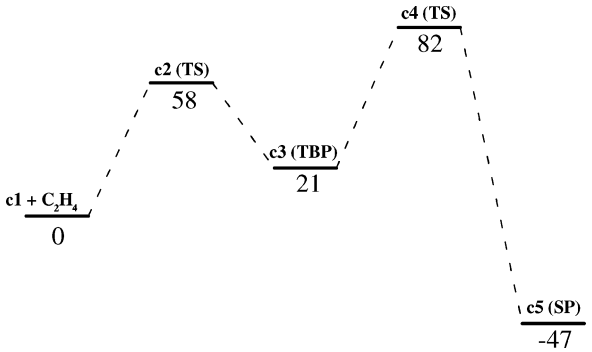

Figure 9. Energy diagram of ethene metathesis on the Mo−methylidene center **c1**. The relative energies (kJ·mol^{-1}) are obtained from the B3LYP/B//B3LYP/A calculations.

TABLE 4: Selected Mulliken (MPA) and Natural (NPA) Charges for the MoO(CH_2) Fragments, the Frontal Orbital Energy Gaps, the Selected Angles, as Well as Both Reaction (ΔE) and Activation ($\Delta E^{\ddagger}$) Energies of the First Molibdacyclobutane Formation

	a1		**b1**		**c1**	
	MPA	NPA	MPA	NPA	MPA	NPA
q(MoO(CH_2))	0.62	0.90	0.76	0.90	0.78	0.98
$e_{LUMO\_site} - e_{HOMO\_ethene}$ (eV)	3.9		4.9		4.7	
$e_{LUMO\_ethene} - e_{HOMO\_site}$ (eV)	6.7		6.5		6.4	
O2−Mo−O3 angle	77.8		105.9		116.6	
O3−Mo−C1−H1 dihedral angle	−35.8		−47.9		−62.4	
ΔE (kJ·mol^{-1})	−84		5		21	
$\Delta E^{\ddagger}$ (kJ·mol^{-1})			37		58	

positive charge on the $MoOCH_2$ moiety in the case of the **a1** structure, compared to **b1** and **c1**.[28,29] In fact, the tendency is just the opposite (Table 4) and does not explain the calculated differences in reactivity. On the other hand, the presented charges of the $MoOCH_2$ fragment are comparable with those previously calculated for very active Mo−methylidene centers on alumina and they are clearly higher than the charges obtained for the less active centers on γ-Al_2O_3.[28,29]

In Figure 10, the frontal molecular orbitals of the Mo−methylidene centers are presented. In accordance with the previous results,[28,29] the interaction between the respective acceptor orbital of the catalyst (LUMO in the present work)

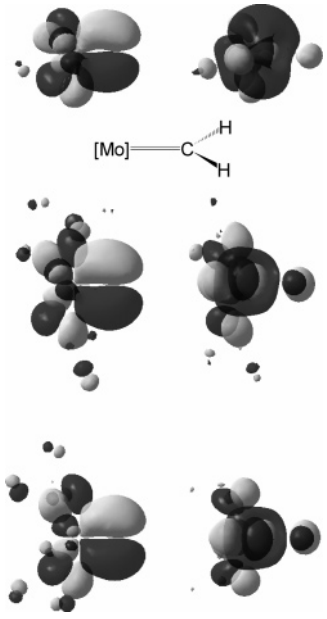

Figure 10. Isosurfaces of the HOMO (left side) and LUMO (right side) of the considered Mo−methylidene centers.

TABLE 5: Calculated and Experimental[55−58] Wavenumbers (cm^{-1}) of the O−H Stretching Vibrations

system	ν^a	system	ν^a
a	3781	**c**	3774
	3783		3783
b	3574[b]	SiO_2 (exp.)	3740−3750
	3788		3720[c]
	3792[c]		3500−3550[d]
	3794		

[a] 0.9929 scaling factor is applied.[100] [b] The H-bonded component of the pair of H-bonded silanols. [c] The free component of the pair of H-bonded silanols. [d] Strongly hydrogen bonded silanols.

and the HOMO of alkene is crucial at the early stage of the molybdacyclobutane formation. The shapes and sizes of the HOMOs of the catalysts, shown in Figure 10, are very similar each other, while the LUMO of **a1** differs significantly from the LUMO of **b1** and **c1**. This suggests that electron donation from the HOMO of ethene to the LUMO of the active site is facilitated for **a1**, compared to both **b1** and **c1** cases. The shape of the LUMO of **a1** also indicates that one side of the carbene bond plane is preferential for a nucleophilic attack. The attack on this side corresponds to formation of the **a2** molybdacyclobutane (Figure 3). The calculated energy gap between the HOMO of ethene and the LUMO of **a1** is lower by about 1 eV than the corresponding differences for **b1** and **c1** (Table 4). On the other hand, the predicted gaps between the HOMO of the Mo−methylidene and the LUMO of ethene are higher and similar to each other for all the centers. Previously, it was shown for Mo−methylidene surface complexes on alumina[28,29] that their reactivity toward alkene is related to the energy difference between the HOMO of ethene and the respective acceptor orbital of the Mo site, too. Thus, the present analysis of the frontal molecular orbitals justifies the high activity of the **a1** site toward ethene, but it does not explain differences in reactivities between the **b1** and **c1** centers.

However, the reactivity order can be also discussed on the basis of the geometrical parameters of the considered Mo−methylidene sites. As one can see from Table 4, the value of the O2−Mo−O3 angle enlarges, when going from **a1** to **c1**, together with increase of the angle between the planes defined by O3−Mo−C1 and Mo−C1−H1 atoms (see Figures 3, 4, and 7). Taking into account the coplanar position of the Mo−O1 bond and the methylidene group, the lower absolute value of the O3−Mo−C1−H1 dihedral angle means a better exposition of the carbene bond toward alkene. Increase of the absolute value of this angle is connected with a stronger steric hindrance for the nucleophilic addition, caused mainly by the O3 atom. This is fully consistent with the reactivity order of the considered sites.

6. Vibrational Frequencies Analysis

6.1. Surface OH Groups. For estimation of the experimental fundamental frequencies from calculated harmonic frequencies, scaling factors derived for a given level of theory are often applied.[98−100] Therefore, the calculated wavenumbers of the O−H stretching vibrations have been scaled with the factor recommended for the B3LYP/6-31g(d) calculations of inorganic molecules.[100] In Table 5, the theoretical wavenumbers for both considered geminal silanols of cluster **a**, the four geminal silanols of cluster **b**, and both considered single silanols of cluster **c** (Figure 2) are presented and compared with the experimental data. Although one cannot expect high accuracy with applying a generic scaling factor, the obtained values are satisfactorily close to the experimental ones.[55−58]

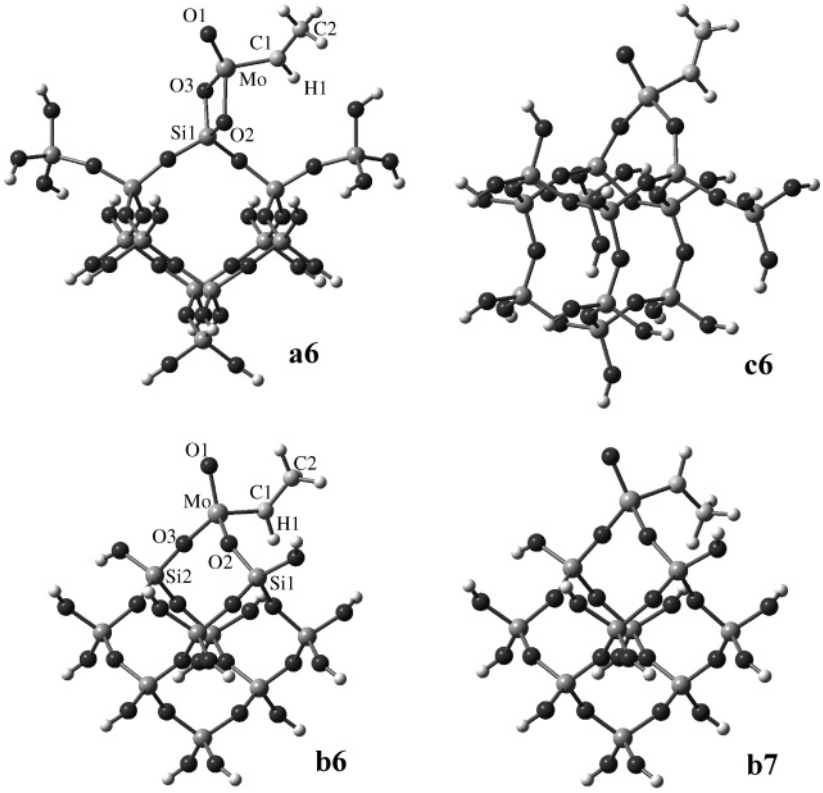

Figure 11. The optimized structures of the Mo−ethylidene centers.

6.2. Mo−Alkylidene and Molybdacyclobutane Centers. There is little direct spectroscopic data concerning surface active sites of the heterogeneous metathesis catalysts. IR spectra of the C−H stretching vibrations of Mo−alkylidene and molybdacyclobutane species generated on SiO_2 were reported by Shelimov and co-workers.[6,7] To compare more experimental and calculated data, structures of Mo−ethylidene centers have been additionally optimized (Figure 11). This species can be present in two stereoisomeric forms. In the case of syn ethylidene, the methyl group points toward the oxo ligand. The other possibility is anti isomer, where the methyl group points away from the oxo ligand. It was previously shown for a similar molybdena−alumina system[90] that the syn species is a little more stable than the anti one. Also in the case of the homogeneous Mo(NAr)-(CHR)$(OR')_2$ Schrock catalyst, the syn isomer is energetically favored.[20−22,101] Therefore, the considered Mo−ethylidene structures **a6**, **b6**, and **c6** are the syn isomers. Additionally, the *anti*-Mo−ethylidene site **b7** has been also optimized (Figure 11). The latter is about 3 kJ·mol^{-1} (ΔE and ΔG) less stable than the syn isomer **b6**. The lower energy of the syn isomer is at least partially explained by an agostic interaction between the Mo atom and the C−H bond in the anti position.[20,21,24,90] A longer C1−H1 bond in **b6** (1.104 Å) than in **b1** (1.097 Å), as well as a decreased value of the Mo−C1−H1 angle in **b6** (110.9°), compared to **b1** (117.7°), suggests existence of the small agostic interaction. In Table 6, other selected geometrical parameters of the Mo−ethylidenes are listed. As one can notice, the geometries are analogous to those of the corresponding Mo−methylidene species (Tables 1−3).

In Table 7, the calculated and scaled wavenumbers of C−H stretching vibrations of the studied Mo−alkylidene and molybdacyclobutane complexes are compared with the experimental data.[6,7] As concerns the molybdacyclobutane centers, six theoretical C−H stretching frequencies are obtained for each of them, whereas only four experimental values were measured. However, on analysis of the plotted theoretical IR spectra (not presented here), based on the calculated vibrational frequencies and intensities, it appears that only four peaks should be observed for each structure, excluding **a2**, where one more peak could be also distinguished. Theoretical wavenumbers, corresponding to these peaks, are italicized in Table 7.

TABLE 6: Selected Bond Lengths (Å) and Angles (deg) for the Mo−Ethylidene Centers

	a6	**b6**	**b7**	**c6**
Mo−C1	1.902	1.898	1.903	1.891
Mo−O1	1.721	1.719	1.718	1.709
Mo−O2	2.015	1.921	1.914	1.970
Mo−O3	1.973	1.901	1.903	1.960
O2−Si1	1.732	1.679	1.675	1.685
O3−Si2[a]	1.741	1.659	1.661	1.684
O2−Mo−O3	77.3	106.1	105.3	117.8
O3−Mo−C1−H1[b]	−29.0	−46.7	−48.5	−62.3

[a] Si1 in the case of **a6**. [b] C2 in the case of **b7**.

On the basis of the vibrational frequencies analysis, one can try to assess which of the proposed active site models is the most similar to the real centers. As a generic scaling factor for the functional and basis sets combination used in the calculations is not given, three different scaling factors (for the **a**, **b**, and **c** series) have been obtained that minimize the root-mean-square deviations of the calculated wavenumbers of the Mo−methylidene and *syn*-Mo−ethylidene centers (Table 7). The wavenumbers for the molybdacyclobutanes were not taken into account, because it was to determine what kind of theoretically obtained intermediate structures, TBP or SP, matches to the experimental data. Although the consistency with the experimental results is quite good for all the proposed structures of the Mo−alkylidenes, it is obvious that the similarity between experiment and theory is much better in the case of the **b** and **c** structures. However, it cannot be said on the basis of these findings, which sites, **b** or **c**, are closer to the real active sites. Concerning the results for the molybdacyclobutane centers, one can state that either the wavenumbers calculated for the **a2**

TABLE 7: The Experimental[6,7] and Calculated Wavenumbers (cm^{-1}) of the C−H Stretching Vibrations

ν_{exp} Mo−methylidene	ν_{calc}[a] a1	b1	c1	ν_{calc}[b] b1
2945	2917	2935	2939	2921
3080	3051	3067	3076	3053

ν_{exp} Mo−ethylidene	ν_{calc}[a] a6	b6	c6	ν_{calc}[b] b7
2850	2865	2858	2854	2845
2890	2905	2895	2897	2911
2910	2929	2921	2917	2958
2985	2994	2986	2979	2973

ν_{exp} molybdacyclobutane	ν_{calc}[a] a2	b3	c3	b5	c5
2870	*2945*	*2958*	*2957*	*2881*	*2886*
2930	*2955*	*2993*	*2993*	*2911*	*2917*
2955	*2999*	2996	2999	2919	2925
2985	*3035*	*3056*	*3054*	*2956*	*2957*
	3053	3096	3100	2995	3002
	3113	*3101*	*3107*	*3003*	*3010*

[a] Scaling factors obtained by a least-squares fit of the Mo-methylidene and *syn*-Mo−ethylidene calculated wavenumbers to the experimental values are used (the 0.9499, 0.9488, and 0.9476 factors for the **a**, **b**, and **c** series, respectively). [b] A scaling factor of 0.9445 obtained by a least-squares fit of the Mo−methylidene **b1** and *anti*-Mo−ethylidene **b7** calculated wavenumbers to the experimental values is used.

structure or those obtained for both TPB intermediates (**b3** and **c3**) do not match to the experimental data. On the other hand, the values calculated for the SP molybdacyclobutanes **b5** and **c5** very well agree with the data obtained for the real catalysts.

Additionally, the factor obtained by a least-squares fit of the calculated wavenumbers of the Mo−methylidene **b1** and *anti*-Mo−ethylidene **b7** to the respective experimental values has been applied to scale the frequencies calculated for **b1** and **b7** (the last column of Table 7). As one can notice, the consistency between the theoretical results and the experimental data is clearly worse than that in the case when the *syn*-Mo−ethylidene **b6** is taken into account.

Thus, on the basis of the vibrational frequencies analysis, it can be concluded that in the active sites detected on the molybdena−silica catalysts by IR spectroscopy,[6,7] the molybdenum is probably not connected via two oxygen bridges with one silica atom. As concerns Mo−ethylidene species, the syn isomers seem to predominate on the surface. It is also shown that the experimentally characterized molybdacyclobutane species are the stable square pyramidal forms, not the very reactive trigonal bipyramidal intermediates, playing a crucial role in the catalytic process.

7. Relative Stability of the Mo−Alkylidene Sites

To estimate the relative stabilities of the Mo alkylidene centers studied, the hypothetical reaction shown in Scheme 1 has been considered. For this purpose, the geometries of the $Mo(O)(CH_2)(OH)_2$ and *syn*-$Mo(O)(CHCH3)(OH)_2$ complexes, as well as the water molecule, have been additionally optimized. As the support, the relaxed silica models **a**, **b**, and **c** (Figure 2) were taken.

The calculated energy and Gibbs free energy changes for the reaction in Scheme 1 are presented in Table 8. As one can see, the obtained values differ significantly. The most thermodynamically stable are **b1** and **b6** sites, while the Mo−alkylidenes **a1** and **a6** are the less stable. For each cluster model of silica

SCHEME 1

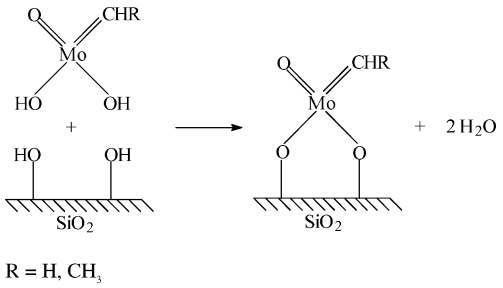

TABLE 8: Calculated (B3LYP/B//B3LYP/A) Relative Stabilities ($kJ \cdot mol^{-1}$) of the Mo−Alkylidene Centers, According to Scheme 1

	a1	a6	b1	b6	c1	c6
ΔE	123	121	−15	−15	73	69
ΔG	100	100	−40	−38	42	48

(**a**, **b**, and **c**), there is practically no difference between the relative stability of the Mo−methylidene and the corresponding Mo−ethylidene center.

In the real catalyst, the Mo−alkylidene structures are usually generated from adequate precursors, after contact with alkene or cycloalkane.[1,3−13] The precursors are formed during a complex and multistage procedure of catalyst preparation and pretreatment. Thus, many factors can influence the final location and structure of the active sites, among them the kinetic factors especially. Therefore, on the basis of the relative energies of the surface Mo−alkylidene complexes it cannot be unequivocally concluded which of them is the best model of the real active sites. However, taking into account the calculated metathesis activities of the considered sites, together with their relative stabilities obtained and vibrational frequencies analysis performed, it can be postulated that the centers replacing two silanols from adjacent geminal pairs are most similar to the real active sites. On the other hand, the simultaneous presence of different sites of different activity on the catalyst cannot be excluded.

8. Conclusions

Ethene metathesis proceeding on Mo−methylidene centers on silica has been studied with DFT, applying the cluster approach to model a silica surface. Three different locations of the active sites have been considered, with the Mo center replacing a pair of geminal silanols, two silanols from adjacent geminal pairs, and two single silanols, respectively. It is shown that metathesis activity of the Mo−methylidene sites strongly depends on their location on silica. Different activities of the considered Mo−methylidene species toward alkene are explained by both their geometrical and electronic structure parameters. The present calculation results are in accordance with the reported high activity of the molybdena−silica systems in olefin metathesis and with experimentally determined values of the activation energy of the reaction.

In two of the three studied cases, the unstable trigonal bipyramidal molybdacyclobutane is initially formed after addition of ethene to the Mo−methylidene center. Then, the trigonal bipyramidal intermediate can decompose to the metathesis product and a new Mo−methylidene site or rearrange to the stable square pyramidal molybdacyclobutane. The latter transformation is kinetically unfavored, in contrast to the previous results obtained for the molybdena−alumina system. Comparison between the calculated vibrational frequencies and reported IR data suggests that the square pyramidal molybda-

cyclobutane complexes are the molybdacyclobutane species detected on the catalyst surface.

On the basis of the calculated metathesis activity of the Mo−methylidene sites, vibrational frequencies analysis for the Mo−methylidene, Mo−ethylidene, and molybdacyclobutane surface complexes, as well as the calculated relative stabilities of the Mo−alkylidene structures, it can be concluded that the Mo centers replacing two silanols from adjacent geminal pairs are, among the studied cases, the most adequate models of the active sites.

Acknowledgment. This work has been supported by Polish Ministry of Science and Information Society Technologies, projects 4 T09A 056 23 (2002-2004) and 3 T09A 093 28 (2005-2006). Computing resources from Academic Computer Centre CYFRONET, AGH University of Science and Technology (Grant No. MNiI/SGI2800/PK/001/2005), are gratefully acknowledged.

References and Notes

(1) Ivin, K. J.; Mol, J. C. *Olefin Metathesis and Metathesis Polymerization*; Academic Press: London, 1997.
(2) Mol, J. C. *J. Mol. Catal. A*: *Chem.* **2004**, *213*, 39.
(3) Iwasawa, Y.; Kubo, H.; Hamamura, H. *J. Mol. Catal.* **1985**, *28*, 191.
(4) Shelimov, B. N.; Elev, I. V.; Kazansky, V. B. *J. Catal.* **1986**, *98*, 70.
(5) Shelimov, B. N.; Elev, I. V.; Kazansky, V. B. *J. Mol. Catal.* **1988**, *46*, 187.
(6) Vikulov, K. A.; Elev, I. V.; Shelimov, B. N.; Kazansky, V. B. *J. Mol. Catal.* **1989**, *55*, 126.
(7) Vikulov, K. A.; Shelimov, B. N.; Kazansky, V. B. *J. Mol. Catal.* **1991**, *65*, 393.
(8) Vikulov, K. A.; Shelimov, B. N.; Kazansky, V. B. *J. Mol. Catal.* **1992**, *72*, 1.
(9) Vikulov, K. A.; Shelimov, B. N.; Kazansky, V. B. *J. Mol. Catal.* **1992**, *72*, 117.
(10) Vikulov, K. A.; Shelimov, B. N.; Kazansky, V. B.; Mol, J. C. *J. Mol. Catal.* **1994**, *90*, 61.
(11) Mol, J. C. *J. Mol. Catal.* **1994**, *90*, 185.
(12) Zhuang, Q.; Fukuoka, A.; Fujimoto, T.; Tanaka, K.; Ichikawa, M. *J. Chem. Soc., Chem. Commun.* **1991**, 745.
(13) Ookoshi, T.; Onaka, M. *Chem. Commun.* **1998**, 2399.
(14) Hèrisson, J.-L.; Chauvin, Y. *Makromol. Chem.* **1971**, *141*, 161.
(15) Katz, T. J.; Rothchild, R. *J. Am. Chem. Soc.* **1976**, *98*, 2519.
(16) Schrock, R. R.; Murdzek, J. S.; Bazan, G. C.; Robbins, J.; DiMare, M.; O'Regan, M. *J. Am. Chem. Soc.* **1990**, *112*, 3875.
(17) Bazan, G. C.; Khosravi, E.; Schrock, R. R.; Feast, W. J.; Gibson, V. C.; O'Regan, M. B.; Thomas, J. K.; Davis, W. M. *J. Am. Chem. Soc.* **1990**, *112*, 8378.
(18) Bazan, G. C.; Oskam, J. H.; Cho, H.-N.; Park, L. Y.; Schrock, R. R. *J. Am. Chem. Soc.* **1991**, *113*, 6899.
(19) Feldman, J.; Schrock, R. R. in *Progress in Inorganic Chemistry*; Lippard, S. J., Ed.; John Wiley & Sons: 1991; Vol. 39, pp 1−74.
(20) Schrock, R. R. In *Topics in Organometallic Chemistry. Alkene Metathesis in Organic Synthesis*; Fürstner, A., Ed.; Springer: Berlin, 1998; Vol. 1, pp 1−36.
(21) Schrock, R. R.; Hoveyda, A. H. *Angew. Chem., Int. Ed.* **2003**, *42*, 4592.
(22) Schrock, R. R. *J. Mol. Catal. A*: *Chem.* **2004**, *213*, 21.
(23) Folga, E.; Ziegler, T. *Organometallics* **1993**, *12*, 325.
(24) Wu, Y.-D.; Peng, Z.-H. *J. Am. Chem. Soc.* **1997**, *119*, 8043.
(25) Wu, Y.-D.; Peng, Z.-H. *Inorg. Chim. Acta* **2003**, *345*, 241.
(26) Hu, A.; Neyman, K. M.; Staufer, M.; Belling, T.; Gates, B. C.; Rösch, N. *J. Am. Chem. Soc.* **1999**, *121*, 4522.
(27) Goursot, A.; Coq, B.; Fajula, F. *J. Catal.* **2003**, *216*, 324.
(28) Handzlik, J. *Surf. Sci.* **2004**, *562*, 101.
(29) Handzlik, J.; Ogonowski, J.; Tokarz-Sobieraj, R. *Catal. Today* **2005**, *101*, 163.
(30) Iwasawa, Y.; Nakano, Y.; Ogasawara, S. *J. Chem. Soc., Faraday Trans. 1* **1978**, *74*, 2968.
(31) Iwasawa, Y.; Ogasawara, S. *J. Chem. Soc., Faraday Trans. 1* **1979**, *75*, 1465.
(32) Iwasawa, Y.; Yamagishi, M. *J. Catal.* **1983**, *82*, 373.
(33) Marcinkowska, K.; Rodrigo, L.; Kaliaguine, S.; Roberge, P. C. *J. Mol. Catal.* **1985**, *33*, 189.
(34) Marcinkowska, K.; Rodrigo, L.; Kaliaguine, S.; Roberge, P. C. *J. Catal.* **1986**, *97*, 75.
(35) Ono, T.; Anpo, M.; Kubokawa, Y. *J. Phys. Chem.* **1986**, *90*, 4780.
(36) Anpo, M.; Kondo, M.; Kubokawa, Y.; Louis, C.; Che, M. *J. Chem. Soc., Faraday Trans. 1* **1988**, *84*, 2771.
(37) Anpo, M.; Kondo, M.; Coluccia, S.; Louis, C.; Che, M. *J. Am. Chem. Soc.* **1989**, *111*, 8791.
(38) Liu, T.; Forissier, M.; Coudurier, G.; Védrine, J. C. *J. Chem. Soc., Faraday Trans. 1* **1989**, *85*, 1607.
(39) Desikan, A. N.; Huang, L.; Oyama, S. T. *J. Phys. Chem.* **1991**, *95*, 10050.
(40) Louis, C.; Che, M.; Anpo, M. *J. Catal.* **1993**, *141*, 453.
(41) Takenaka, S.; Tanaka, T.; Funabiki, T.; Yoshida, S. *J. Phys. Chem. B* **1998**, *102*, 2960.
(42) Radhakrishnan, R.; Reed, C.; Oyama, S. T.; Seman, M.; Kondo, J. N.; Domen, K.; Ohminami, Y.; Asakura, K. *J. Phys. Chem. B* **2001**, *105*, 8519.
(43) Bañares, M. A.; Hu, H.; Wachs, I. E. *J. Catal.* **1994**, *150*, 407.
(44) Hu, H.; Wachs, I. E.; Bare, S. R. *J. Phys. Chem.* **1995**, *99*, 10897.
(45) Mestl, G.; Srinivasan, T. K. K. *Catal. Rev.—Sci. Eng.* **1998**, *40*, 451.
(46) Wachs, I. E. *Top. Catal.* **1999**, *8*, 57.
(47) Zhang, B.; Li, Y.; Lin, Q.; Jin, D. *J. Mol. Catal.* **1988**, *46*, 229.
(48) Zhang, B.; Liu, N.; Lin, Q.; Jin, D. *J. Mol. Catal.* **1991**, *65*, 15.
(49) Kuznetsov, B. N.; Startsev, A. N.; Yermakov, Yu. I. *J. Mol. Catal.* **1980**, *8*, 135.
(50) Sindorf, D. W.; Maciel, G. E. *J. Am. Chem. Soc.* **1983**, *105*, 1487.
(51) Chuang, I.-S.; Kinney, D. R.; Bronnimann, Ch. E.; Zeigler, R. C.; Maciel, G. E. *J. Phys. Chem.* **1992**, *96*, 4027.
(52) Kinney, D. R.; Chuang, I.-S.; Maciel, G. E. *J. Am. Chem. Soc.* **1993**, *115*, 6786.
(53) Chuang, I.-S.; Kinney, D. R.; Maciel, G. E. *J. Am. Chem. Soc.* **1993**, *115*, 8695.
(54) Chuang, I.-S.; Maciel, G. E. *J. Am. Chem. Soc.* **1996**, *118*, 401.
(55) Chuang, I.-S.; Maciel, G. E. *J. Phys. Chem. B* **1997**, *101*, 3052.
(56) Morrow, B. A.; McFarlan, A. J. *J. Non-Cryst. Solids* **1990**, *120*, 61.
(57) Morrow, B. A.; McFarlan, A. J. *J. Phys. Chem.* **1992**, *96*, 1395.
(58) Haukka, S.; Lakomaa, E.-L.; Root, A. *J. Phys. Chem.* **1993**, *97*, 5085.
(59) Hirva, P.; Pakkanen, T. A. *Surf. Sci.* **1992**, *271*, 530.
(60) Hsu, L.-Y.; Shore, S. G.; D'Ornelas, L.; Choplin, A.; Basset, J.-M. *J. Catal.* **1994**, *149*, 159.
(61) Shay, T. B.; Hsu, L.-Y.; Basset, J.-M.; Shore, S. G. *J. Mol. Catal.* **1994**, *86*, 479.
(62) Vigné-Maeder, F.; Sautet, P. *J. Phys. Chem. B* **1997**, *101*, 8197.
(63) Verpoort, F.; Bossuyt, A. R.; Verdonck, L.; Coussens, B. *J. Mol. Catal. A*: *Chem.* **1997**, *115*, 207.
(64) Branda, M. M.; Castellani, N. J. *Surf. Sci.* **1997**, *393*, 171.
(65) Ferreira, M. L.; Branda, M. M.; Juan, A.; Damiani, D. E. *J. Mol. Catal. A*: *Chem.* **1997**, *122*, 51.
(66) Mortensen, J. J.; Parrinello, M. *J. Phys. Chem. B* **2000**, *104*, 2901.
(67) Suvanto, S.; Hirva, P.; Pakkanen, T. A. *Surf. Sci.* **2000**, *465*, 277.
(68) Griffe, B.; Sierraalta, A.; Ruette, F.; Brito, J. L. *J. Mol. Catal. A*: *Chem.* **2001**, *168*, 265.
(69) Ferreira, M. L.; Volpe, M. *J. Mol. Catal. A*: *Chem.* **2002**, *184*, 349.
(70) Ma, Q.; Klier, K.; Cheng, H.; Mitchell, J. W. *J. Phys. Chem. B* **2002**, *106*, 10121.
(71) Griffe, B.; Sierraalta, A.; Ruette, F.; Brito, J. L. *J. Mol. Struct. (THEOCHEM)* **2003**, *625*, 59.
(72) Peacor, D. R. *Z. Kristallogr.* **1973**, *138*, 274.
(73) Hua, G. L.; Welberry, T. R.; Withers, R. L.; Thompson, J. G. *J. Appl. Crystallogr.* **1988**, *21*, 458.
(74) Welberry, T. R.; Hua, G. L.; Withers, R. L. *J. Appl. Crystallogr.* **1989**, *22*, 87.
(75) Wright, A. F.; Leadbetter, A. J. *Philos. Mag.* **1975**, *31*, 1391.
(76) O'Keeffe, M.; Hyde, B. G. *Acta Crystallogr., Sect. B* **1976**, *32*, 2923.
(77) Becke, A. D. *J. Chem. Phys.* **1993**, *98*, 5648.
(78) Stevens, P. J.; Devlin, J. F.; Chabalowski, C. F.; Frisch, M. J. *J. Phys. Chem.* **1994**, *98*, 11623.
(79) Frisch, M. J.; Trucks, G. W.; Schlegel, H. B.; Scuseria, G. E.; Robb, M. A.; Cheeseman, J. R.; Montgomery, J. A., Jr.; Vreven, T.; Kudin, K. N.; Burant, J. C.; Millam, J. M.; Iyengar, S. S.; Tomasi, J.; Barone, V.; Mennucci, B.; Cossi, M.; Scalmani, G.; Rega, N.; Petersson, G. A.; Nakatsuji, H.; Hada, M.; Ehara, M.; Toyota, K.; Fukuda, R.; Hasegawa, J.; Ishida, M.; Nakajima, T.; Honda, Y.; Kitao, O.; Nakai, H.; Klene, M.; Li, X.; Knox, J. E.; Hratchian, H. P.; Cross, J. B.; Bakken, V.; Adamo, C.; Jaramillo, J.; Gomperts, R.; Stratmann, R. E.; Yazyev, O.; Austin, A. J.; Cammi, R.; Pomelli, C.; Ochterski, J. W.; Ayala, P. Y.; Morokuma, K.; Voth, G. A.; Salvador, P.; Dannenberg, J. J.; Zakrzewski, V. G.; Dapprich, S.; Daniels, A. D.; Strain, M. C.; Farkas, O.; Malick, D. K.; Rabuck, A. D.; Raghavachari, K.; Foresman, J. B.; Ortiz, J. V.; Cui, Q.; Baboul, A.

G.; Clifford, S.; Cioslowski, J.; Stefanov, B. B.; Liu, G.; Liashenko, A.; Piskorz, P.; Komaromi, I.; Martin, R. L.; Fox, D. J.; Keith, T.; Al-Laham, M. A.; Peng, C. Y.; Nanayakkara, A.; Challacombe, M.; Gill, P. M. W.; Johnson, B.; Chen, W.; Wong, M. W.; Gonzalez, C.; Pople, J. A. *Gaussian 03*, Revision C.02; Gaussian, Inc.: Wallingford, CT, 2004.

(80) Hay, P. J.; Wadt, W. R. *J. Chem. Phys.* **1985**, *82*, 299.

(81) Dunning, T. H., Jr.; Hay, P. J. In *Modern Theoretical Chemistry*; Schaefer, H. F., III, Ed.; Plenum: New York, 1976; Vol. 3, pp 1−28.

(82) Peng, C.; Ayala, P. Y.; Schlegel, H. B.; Frisch, M. J. *J. Comput. Chem.* **1996**, *17*, 49.

(83) Mulliken, R. S. *J. Chem. Phys.* **1955**, *23*, 1833, 1841, 2338, 2343.

(84) Reed, A. E.; Curtiss, L. A.; Weinhold, F. *Chem. Rev.* **1988**, *88*, 899.

(85) Glendening, E. D.; Reed, A. E.; Carpenter, J. E.; Weinhold, F. NBO Version 3.1.

(86) Mayer, I. *Chem. Phys. Lett.* **1983**, *97*, 270.

(87) Cundari, T. R.; Gordon, M. S. *J. Am. Chem. Soc.* **1991**, *113*, 5231.

(88) Rappé, A. K.; Goddard, W. A., III *J. Am. Chem. Soc.* **1982**, *104*, 448.

(89) Handzlik, J.; Ogonowski, J. *J. Mol. Catal. A*: *Chem.* **2002**, *184*, 371.

(90) Handzlik, J. *J. Catal.* **2003**, *220*, 23.

(91) Handzlik, J. *J. Mol. Catal. A*: *Chem.* **2004**, *218*, 91.

(92) Davie, E. S.; Whan, D. A.; Kemball, C. *J. Catal.* **1972**, *24*, 272.

(93) Grünert, W.; Stakheev, A. Yu.; Feldhaus, R.; Anders, K.; Shpiro, E. S.; Minachev, Kh. M. *J. Catal*. **1992**, *135*, 287.

(94) Handzlik, J.; Ogonowski, J. in *Technologia chemiczna na przełomie wieków*, Wydawnictwo Stałego Komitetu Kongresów Technologii Chemicznej: Gliwice, 2000, pp 149−152. (The abstract in "3rd Congress of Chemical Technology: The Chemical Technology at the Change of the Century. Abstracts of Lectures, Oral Communications and Posters", p 44. A Publication of the Permanent Committee of the Congresses of Chemical Technology, Gliwice 2000).

(95) Yi, W.; Schwidder, M.; Grünert, W. *Catal. Lett.* **2003**, *86*, 113.

(96) Moffat, A. J.; Clark, A. *J. Catal.* **1970**, *17*, 264.

(97) Kapteijn, F.; Bredt, H. L. G.; Homburg, E.; Mol, J. C. *Ind. Eng. Chem. Prod. Res. Dev.* **1981**, *20*, 457.

(98) Scott, A. P.; Radom, L. *J. Phys. Chem.* **1996**, *100*, 16502.

(99) Wong, M. W. *Chem. Phys. Lett.* **1996**, *256*, 391.

(100) Bytheway, I.; Wong, M. W. *Chem. Phys. Lett.* **1998**, *282*, 219.

(101) Oskam, J. H.; Schrock, R. R. *J. Am. Chem. Soc.* **1993**, *115*, 11831.